Two-Layer Model of Turbulent Boundary Layers

BARRY L. REEVES*
Avco Systems Division, Wilmington, Mass.

A small cross-flow model of two- and three-dimensional compressible turbulent boundary layers is developed which is based on an explicit inner-outer layer approach. The lateral extent of the inner (wall) layer is treated as a separate length scale and is found as one of the dependent variables of a system of ordinary differential equations in the streamwise direction. It is shown that the interaction of the inner and outer layers and thus the whole history of the flow determines this length scale. Results of the model have been compared with a number of experiments for flows in strong positive and negative pressure gradients and flows with surface mass injection. Results are presented here for several flows with rapid departures from fluid dynamic equilibrium, including the approach to separation.

Nomenclature

a = sonic velocity
a^* = $(1-\bar{U}_m)$
A^2 = parameter in Crocco integral for wall layer, Eq. (24)
B = parameter in Crocco integral for wall layer, Eq. (25)
$\bar{B}$ = empirical "constant" in law of the wall
C_f = skin-friction coefficient, Eq. (38), $\tilde{C}_f = 2C_f$
C_f' = $(u_\tau/u_e)^2$ or $(h_w/h_e)C_f$
C_H = Stanton number
C_p = specific heat at constant pressure
F = inverse turbulent Reynolds number in outer layer, Eq. (48)
h = static enthalpy
h^+ = h/h_w
H = stagnation enthalpy
$\bar{H}$ = H/H_e
J_i = flux integrals in inner layer, Eqs. (30, 31, 33, and 34)
K = empirical constant in law of the wall, $K = 0.41$
l = mixing length
L = reference length in coordinate transformation, Eq. (6)
M_e = Mach number at edge of boundary layer
m = exponent of stagnation enthalpy profiles in outer layer, Eq. (36)
m_e = $[(\gamma-1)/2]M_e^2$
m = mass flux in inner layer
M = surface mass injection parameter $\rho_w \tilde{v}_w/\rho_e \tilde{u}_e$
n = exponent of velocity profiles in outer layer, Eq. (35)
p = static pressure
Pr_t = turbulent Prandtl number
q = heat flux
$r(\bar{x})$ = spreading metric of inviscid streamlines
Re_y = $y^+/(u_\tau/u_e)$
St = modified Stanton number, Eq. (37)
$\tilde{u}, \tilde{v}$ = velocity components in physical coordinates $\tilde{x}$, $\tilde{y}$, respectively
u, v = velocity components in transformed, "two-dimensional" coordinates x, y, respectively
U, V = velocity components in transformed, constant density coordinates X, Y, respectively
$\bar{U}$ = U/U_e
$\tilde{u}^+$ = $\tilde{u}/\tilde{u}_\tau$
$\tilde{u}_\tau$ = friction velocity, $(\tau_w/\rho_w)^{1/2}$
$\tilde{y}_m$ = thickness of inner layer (match point)
$\tilde{y}^+$ = $\tilde{u}_\tau \tilde{y}/\nu_w$
γ = ratio of specific heats
δ = thickness of outer layer in transformed, constant density coordinates X, Y
δ_e = thickness of boundary layer (two-dimensional)
δ_i^* = "incompressible" displacement thickness
δ^* = displacement thickness (two-dimensional)
$\tilde{\delta}_e, \tilde{\delta}^*$ = thickness and displacement thickness in physical coordinates
ε = turbulent eddy viscosity
σ = exponent in temperature viscosity law, $\mu \sim T^\sigma$
η = normalized coordinate in outer layer, Eq. (39)
θ = momentum thickness (two-dimensional)
$\tilde{\theta}$ = momentum thickness in physical coordinates
μ = viscosity
ν = kinematic viscosity
ξ = $\tilde{u}/\tilde{u}_e$
ρ = density
τ = stress
ψ = stream function
ω = exponent in eddy viscosity variation across outer layer, Eq. (46)

Subscripts

e = edge of boundary layer
m = at match point y_m
o = isentropic stagnation conditions behind normal shock, also initial conditions
s = local stagnation conditions at edge of layer
w = wall conditions

Presented as Paper 73-135 at the AIAA 11th Aerospace Sciences Meeting, Washington, D.C., January 10–12, 1973; submitted March 8, 1973; revision received December 13, 1973. The author expresses his appreciation to H. Baum and D. Siegelman for helpful discussions, and to H. Buss for writing the computer program and assisting with some of the computations. This research was sponsored by the Advanced Research Projects Agency of the Department of Defense and by the Space and Missile Systems Organization, Air Force Systems Command.

Index categories: Boundary Layers and Convective Heat Transfer—Turbulent; Supersonic and Hypersonic Flow.

* Senior Consulting Scientist.

I. Introduction

ACCURATE prediction of turbulent boundary layers about re-entry bodies is of critical importance in calculating wall friction and heat transfer, observables, communication (guidance and telemetry), and re-entry aerodynamics in general. Recently, interest in maneuvering and lifting re-entry vehicles and advanced nosetips has placed added emphasis on developing a method capable of predicting two- and three-dimensional turbulent boundary layers in which there are strong and rapid departures from fluid dynamic equilibrium.

This paper describes a two-layer model developed for this purpose in which an analytical solution for the inner layer, based on a compressible law of the wall, is matched with a moment integral method for the outer layer. The essence of the model lies in the partitioning of the turbulence production $-\overline{(\rho v)'u'}(\partial u/\partial y)$ between the inner and outer layers, allowing the flow to be computed as an inner and outer layer interaction problem. This interaction is what ultimately determines the length scale of the inner layer $\tilde{y}_m$. In the two-layer model $\tilde{y}_m$ is one of the dependent variables of a system of differential equations in the streamwise direction $\tilde{x}$, and it depends on the whole history of the flow. Thus, $\tilde{y}_m$ is treated as a separate length scale of the boundary layer which is just as crucial to the dynamics of the layer as the over-all momentum and displacement thicknesses.

The physical basis for dividing the layer into inner and outer layers, with appropriate matching conditions along the common interface $\tilde{y}_m$, is the experimental demonstration that even in highly nonequilibrium flows there exists an inner layer in which turbulence production balances dissipation. The velocity and enthalpy profiles in this inner layer are accurately described by a generalized law of the wall, which includes effects of heat transfer, compressibility, and surface mass injection.[1] In terms of mean flow velocity and enthalpy profiles $\tilde{y}_m$ is the point in the layer where the law of the wall breaks down and turbulence production no longer balances dissipation. For highly nonequilibrium flows, the two-layer model predicts that (u/u_e) along the match point, and the relative scale of the inner layer $(\tilde{y}_m/\tilde{\delta}_e)$ itself, are rapidly varying functions of streamwise distance $\tilde{x}$. At separation, for example, which now can be predicted by the model if the pressure distribution is prescribed, $\tilde{C}_f \to 0$, $\tilde{y}_m/\tilde{\delta}_e \to 0$ and $(u/u_e)_m \to 0$ so that the boundary layer is dominated by the outer layer (or by the "wake component" in the terminology of Coles[2]). One of the unique features of the model is that the stability of the system of ordinary differential equations can be used to establish upper and lower bounds on the turbulent production integral $\int \tau\, du$ in the outer layer. Stable solutions up to Mach 10 for a wide range of wall-to-freestream temperature ratios, pressure gradients, and surface mass transfer rates show that compressibility has little effect on the properly normalized lateral stress profiles, confirming some observations of Maise and McDonald.[3]

In Ref. 4, it was shown that the generalized law of the wall can be inserted into the full conservation equations, which are then integrated to find the stress $\tau(y)$ and heat flux $q(y)$ distributions across the inner layer. The conservation equations are satisfied exactly in the inner layer, and τ and q are "unhooked" from a simple local determination via the mixing length and velocity gradient. As we will show, this "unhooking" of the stress and heat flux from local quantities is essential for accurate calculations of highly nonequilibrium boundary layers.

II. Turbulent Boundary-Layer Model

Equations of Motion and Coordinate Systems

If the boundary-layer equations are written following inviscid streamlines and the cross flow in the boundary layer normal to the local inviscid streamline direction can be assumed small, the mean flow equations are

$$(\partial/\partial\tilde{x})(\rho\tilde{u}r)+(\partial/\partial\tilde{y})(\rho\tilde{v}r)=0 \tag{1}$$

$$\rho\tilde{u}\,\partial\tilde{u}/\partial\tilde{x}+\rho\tilde{v}\,\partial\tilde{u}/\partial\tilde{y}=-dp_e/d\tilde{x}+\partial\tau/\partial\tilde{y} \tag{2}$$

$$\rho\tilde{u}\,\partial H/\partial\tilde{x}+\rho\tilde{v}\,\partial H/\partial\tilde{y}=(\partial/\partial\tilde{y})(q+\tilde{u}\tau) \tag{3}$$

where $r(\tilde{x})$ is the spreading metric determined by the inviscid flow streamline geometry. The uncoupled small cross-flow momentum equation is neglected, and it is assumed that the additional contributions to turbulent stress and heat flux resulting from fluctuations in the cross-flow velocity are small as well. Thus,

$$\tau=\mu\,\partial\tilde{u}/\partial\tilde{y}-\overline{(\rho v)'u'} \tag{4}$$

and

$$q=k\,\partial h/\partial\tilde{y}-\overline{(\rho v)'h'} \tag{5}$$

Clearly, for a body at large angle of attack, these stress and heat flux models will break down on the leeward side because strong cross flows with additional contributions to the Reynolds stress have to be included, along with interaction with the outer flow.[4]

The explicit appearance of the spreading metric in the equations of motion can be eliminated by means of a modified Mangler transformation. Although it turns out that $r(\tilde{x})$ later appears in a constant of integration in the compressible law of the wall, the transformation is convenient since it is possible to remove r from the continuity equation without transforming the stress or heat flux. Letting

$$dx=[r(\tilde{x})/L]\,d\tilde{x}; \qquad dy=[r(\tilde{x})/L]\,d\tilde{y} \tag{6}$$

with

$$u=\tilde{u}; \quad v=\tilde{v}+\tilde{u}\tilde{y}\,d(\ln r)/d\tilde{x} \tag{7}$$

Equations (1–3) become

$$\partial(\rho u)/\partial x+\partial(\rho v)/\partial y=0 \tag{8}$$

$$\rho u\frac{\partial u}{\partial x}+\rho v\frac{\partial u}{\partial y}=-\frac{dp_e}{dx}+\frac{\partial\tau}{\partial y} \tag{9}$$

$$\rho u\frac{\partial H}{\partial x}+\rho v\frac{\partial H}{\partial y}=\frac{\partial}{\partial y}(q+u\tau) \tag{10}$$

where τ and q are still defined by Eqs. (4) and (5). Solution of the inner layer is obtained directly using Eqs. (8–10) without further transformation of the coordinates to remove the explicit appearance of the density. The reason for this is twofold. First, within the framework of the present model for the inner layer an analytic solution can be obtained without introducing a compressibility transformation. Second, Maise and McDonald[3] have shown that a compressibility transformation leads to generally poor results for the turbulent stress distributions across the boundary layer even for constant pressure adiabatic flows. They also showed poor correlation of experimental velocity profiles using the transformation for constant pressure flows with heat transfer. More recently, Lewis et al.[5] attempted to generalize Coles' transformation but they also found significant deviation between experimental velocity profiles and profiles predicted using the transformation, especially in the wall layer. They showed that the discrepancy between profiles increased with increasing Mach number so that for flow on a flat plate at Mach 6, for example, a difference of 20% in velocity profiles can be expected. The reason for this is that conventional compressibility transformations cannot give the proper scaling to reproduce the generalized law of wall in the inner layer. The only transformation which can accomplish this is given by $du=(\bar{\rho}/\rho)^{1/2}\,dU$, but this fails in the outer layer.

In the outer wakelike layer, however, where we use an integral moment method, a compressibility transformation is used merely to remove the explicit appearance of the density from Eqs. (8–10). This can be accomplished without transforming the stress and heat flux by letting

$$dX=dx, \quad dY=(a_e/a_o)(\rho/\rho_o)\,dy \tag{11}$$

$$\Psi=\psi, \quad U=(a_o/a_e)u$$
$$V=(\rho/\rho_o)v+U(\partial Y/\partial x) \tag{12}$$

so that Eqs. (8–10) become

$$\partial U/\partial X+\partial V/\partial Y=0 \tag{13}$$

$$U\frac{\partial U}{\partial X}+V\frac{\partial U}{\partial Y}=(H/H_e)U_e\frac{dU_e}{dX}+\frac{a_o}{a_e\rho_o}\frac{\partial\tau}{\partial Y} \tag{14}$$

$$U\frac{\partial H}{\partial X}+V\frac{\partial H}{\partial Y}=\frac{1}{\rho_o}\frac{\partial}{\partial Y}\left(q+\frac{a_e}{a_o}U\tau\right) \tag{15}$$

Here τ and q are still the physical stress and heat flux defined by Eqs. (4) and (5). We do not require transformation of τ and q to an equivalent low-speed flow. Equations (13–15) are used to develop the integral moment equations for the outer layer.

With the equations of motion and proper coordinate systems developed for the inner and outer layers, we now proceed to the turbulence model used in the two-layer model.

Turbulence Model

In order to develop a scheme for solving Eqs. (1–3), it is necessary to have some knowledge either of the relationships between τ, q and mean flow quantities p, u, H (provided such relationships exist) or have additional independent differential equations for τ and q. Several model transport equations[6,7] for the stress and heat flux based on the latter approach have been developed recently and, hopefully, these will provide new insight into the way the stress and heat flux respond to changes in boundary conditions as the flow proceeds downstream. To date, however, all these approaches using model transport equations for τ and q have had to invoke assumptions for closure of the higher correlation functions whose physical basis has only been

demonstrated in incompressible flows. At moderate Mach numbers, however (up to $M_e \simeq 9$), there is much experimental evidence that the turbulent boundary layer may be divided into an inner wall layer and an outer wake layer, as in incompressible flow. In the wall layer, the properly normalized experimental velocity and enthalpy profiles have been shown to be functions of the local wall stress, heat flux, injection rate, and wall temperature but are virtually independent of the upstream history of the layer.[8,9] This is precisely the result predicted by the thin-layer Couette model which leads to a compressible law of the wall and a Crocco integral for the inner layer. For flows with surface mass injection, Danberg and Squire have shown that this same model accurately predicts the velocity distribution in the wall layer. In fact, the experimental evidence for the Van Driest[10] form of the law of the wall for $M = 0$ and the Squire form of this law for $M \neq 0$ is now so strong that model transport equations for the turbulent stress either "reduce" to this law near the wall or are matched to it. Even for flows in positive or negative pressure gradients, there is experimental evidence that the law of the wall gives an accurate representation of the velocity profile over some distance $\tilde{y}_m$ away from the surface. If we accept the generalized law of the wall as being applicable to flows with surface mass injection and pressure gradient, the remaining questions to be answered insofar as the inner layer is concerned are a) the determination of the lateral stress and heat flux profiles, which are required for matching with the outer layer, and b) calculation of the distance from the surface $\tilde{y}_m$ at which the velocity profile departs from the law of the wall (and where the stagnation enthalpy departs from the linear Crocco integral). Following Coles'[2] analysis for incompressible flows, the stress and heat flux profiles can be found by inserting the wall law into the full momentum and energy equations and integrating these equations away from the surface. In this way the stress and heat flux in the inner layer depend on the past history of the layer, as well as on local properties, and are "unhooked" from a purely local determination through the mixing length and local velocity gradient. Taking this approach, the momentum and energy equations now serve as the transport equations for τ and q.

We now consider the outer layer, where the evaluation of the stress and heat flux is much more questionable. For non-equilibrium flows, it is generally accepted that the stress in the outer layer depends on the whole history of the layer and cannot be found from local mean flow properties. Contrary to the situation for equilibrium layers, the use of an eddy viscosity or mixing length should be held suspect because, in general, there is no simple proportionality between the turbulent stress and mean flow velocity gradient applicable across all the outer layer. It follows, then, that the relative scale of the inner and outer layers $\tilde{y}_m$ cannot be determined simply from the local mixing length and velocity gradient, as is usually assumed in conventional finite-difference methods,[11,12] but it also must respond to the whole history of the flow. In the two-layer model a simple local relation for $\tilde{y}_m$ is avoided by matching the stress obtained from the transport equation in the inner layer with a relation for the stress applicable in the outer layer. By matching the stress resulting from the transport equation along the boundary of the inner and outer layers, and by taking a higher moment of the momentum equation in the outer layer, $\tilde{y}_m$ can be found as one of the integral properties of the layer.

In the present two-layer model a relation for the stress along the match point $\tilde{y}_m$ is required along with a relation for the turbulence production integral across the outer layer

$$\int_{u_m}^{u_e} (\tau/\tau_m)\, du \tag{16}$$

Because the turbulent boundary layer is divided into two more or less distinct layers, which are free to interact, the model can be expected to reveal certain consequences of this inner and outer layer interaction that are not quite so apparent in other methods. Indeed, this turns out to be the case because the two-layer model provides upper and lower bounds on the magnitude of the production integral over the outer layer. If estimates for this integral are made which are too small or too large, integrations of the system of equations downstream develop instabilities in which the inner layer rapidly swallows the outer layer for the former and the outer swallows the inner for the latter. We find that the production integral over the outer layer cannot be assumed negligibly small nor can it be evaluated using a constant eddy viscosity across the outer layer, as was suggested by Clauser.[13] Both assumptions give unstable solutions, although the Clauser assumption is stable for Mach numbers below about 2.5. Thus, the stability of the system of equations, which reflects on the stability of the interaction between the inner and outer layers, provides a means of evaluating the production integral over the outer layer. This is a most useful result because the production integral contains the influence of turbulent intermittency at the boundary-layer edge and the effects of long-time stress "memory" of large eddies in flows which are far from equilibrium. By evaluating the production integral as though the density were constant across the outer layer and by using a cubic variation of ε between $\tilde{y}_m$ and $\tilde{\delta}_e$ with $\varepsilon \to 0$ at the outer edge, stable solutions have been obtained up to Mach 14 for wall to freestream stagnation temperature ratios between 0.05 and 1.0. These results for the bounds on the production integral and the assumptions used to produce stable solutions verify the results of Maise and McDonald who showed that compressibility has little effect on experimental stress profiles (when normalized by the wall stress) up to about Mach 5. A cubic variation of ε for $\tilde{y}_m < \tilde{y} < \tilde{\delta}_e$ is also consistent with ε variations inferred by Maise and McDonald[3] and Bradshaw[14] from various data.

The stress along the match point of the inner and outer layers is evaluated using the eddy viscosity relation

$$\tau_m = \rho_m \varepsilon_m (\partial \tilde{u}/\partial \tilde{y})_m \tag{17}$$

Thus, while the evaluation of τ along $\tilde{y}_m$ is subject to some of the objections of "localness," as we have seen, the location of the match point where τ_m is evaluated depends on the history of the layer.

These aspects of the two-layer model, namely the interaction of inner and outer layers, the determination of $\tilde{y}_m$ as a result of this interaction, and "unhooking" of τ and q from local quantities, are the key features of the turbulence model that distinguish the model from conventional finite-difference methods. A kind of two-layer structure is also implicit in finite-difference methods, but the relative scale of the inner and outer layers is set once and for all by the specification of a universal distribution of the mixing length (or eddy viscosity). Moreover, this universal distribution is usually specified on the basis of experimental data obtained from equilibrium layers or from layers close to equilibrium.[11,12] For example, one of the conventional assumptions is that outside the sublayer, the mixing length increases with $\tilde{y}$ according to $l = 0.41\tilde{y}$ until it attains the value $l = 0.09\tilde{\delta}_e$ in the outer layer. This implies a relative scale for the inner layer of $\tilde{y}_m/\tilde{\delta}_e = 0.22$ independent of the magnitude of the pressure gradient! Both experiments and results computed using the two-layer model have shown that this relative scale is only valid for flows in zero or weak pressure gradients in or near equilibrium. In large positive pressure gradients, the inner layer may become vanishingly small, while in large negative pressure gradients, $\tilde{y}_m$ may be of the order of the boundary-layer thickness.

Although τ is "unhooked" from local quantities in the two-layer model, results of solutions can be used to go back and compute the variation of the mixing length from the formal definition, i.e., from

$$\tau = \rho l^2 (\partial \tilde{u}/\partial \tilde{y})^2 \tag{18}$$

outside the sublayer. The result for the variation of l in the inner layer is

$$l = 0.41\tilde{y}[\tau(\tilde{y})/\tau_w]^{1/2} \tag{19}$$†

† At a separation point ($\tau_w = 0$) the two-layer model predicts that the inner layer vanishes, which is precisely what Coles hypothesized with his law of the wall, law of the wake profiles. Of course, this variation of mixing length away from the surface applies only outside the sublayer.

Thus, while conventional methods assume that l grows as a universal constant times $\tilde{y}$, the two-layer model predicts a nonlinear variation of l with $\tilde{y}$ whenever there are large pressure gradients or rapid departures from fluid dynamic equilibrium. For flows in positive pressure gradients, or for boundary layers relaxing after the sudden removal of a positive pressure gradient, $\tau(y) > \tau_w$ in the inner layer and the mixing length is predicted to increase more rapidly than $0.41\tilde{y}$ away from the surface. This behavior is borne out by the experimental data obtained by Bradshaw and Ferriss[14] (and by the analysis of their data and other data by Glowacki and Chi[15]) and by the data of Sturek and Danberg.[16,17] Bradshaw and Ferriss found that in a constant-pressure boundary layer immediately following the removal of a positive-pressure gradient, $l/\tilde{y}$ was as large as 0.61 in the inner layer.

In their experiments on sudden changes in surface roughness, Antonia and Luxton[18] measured large deviations from $l = 0.41\tilde{y}$ in the inner layer, and they observed a dependence of l on $\tau^{1/2}$.

III. Solution of Inner Layer and Matching Conditions

Using a first-order Couette model of the flow near the wall, a generalized law of the wall for the velocity and enthalpy with surface mass injection is obtained. These velocity and enthalpy profiles are then inserted back into the full continuity, momentum, and energy equations, which are integrated away from the surface to give the stress, heat flux, and mass flux at the outer edge of the inner layer. This operation "unhooks" the stress and heat flux from local quantities such as the velocity and enthalpy gradients and mixing length. The velocity, enthalpy, stress, heat flux, and mass flux at the edge of the wall layer can be obtained analytically, and these expressions, along with certain auxiliary relations for normal and streamwise derivatives of the velocity and enthalpy, are used for matching with the integral method in the outer layer. One of the key features of the present two-layer model is that matching with the outer layer ultimately determines the lateral extent of the wall layer (or, in Coles' terminology, the strength of the wake component); it is not specified in advance in terms of the eddy viscosity or mixing length variation.

With the possible exception of boundary layers in very strong negative pressure gradients, in which the layer may relaminarize, we assume that a wall layer exists where the velocity and enthalpy profiles are closely approximated by a Couette flow model. Treating only the fully turbulent part of the wall layer (in the first approximation) and setting $Pr_t = 1$, the first-order equations for the stress and heat flux, obtained by integrating the momentum and energy equations away from the surface, are

$$\tau(\tilde{y}) = \tau_w + \rho_w \tilde{v}_w \tilde{u} = \rho K^2 \tilde{y}^2 (\partial\tilde{u}/\partial\tilde{y})^2 \tag{20}$$

$$q(\tilde{y}) = q_w - \tilde{u}\tau(\tilde{y}) + \rho_w \tilde{v}_w (H - H_w) = \rho K^2 \tilde{y}^2 (\partial\tilde{u}/\partial\tilde{y})(\partial h/\partial\tilde{y}) \tag{21}$$

Dividing the second equation by the first and integrating the result gives a Crocco integral, which is always valid in the inner layer independent of pressure gradient or surface mass injection

$$H/H_w = 1 + B(\tilde{u}/\tilde{u}_e) \tag{22}$$

where, in general, $B = B(\tilde{x})$. It is only in the special case of zero pressure gradient *equilibrium* layers that Eq. (22) applies in the outer layer as well, and in this case B is constant. Also

$$h/h_w = 1 + B(\tilde{u}/\tilde{u}_e) - A^2(\tilde{u}/\tilde{u}_e)^2 \tag{23}$$

where

$$A^2 = [m_e/(1+m_e)](H_e/H_w) \tag{24}$$

$$B = [2m_e/(1+m_e)](H_e/H_w)(St/C_f) \tag{25}$$

Substituting for $\rho = \rho_w(h_w/h)$ in the expression for $\tau(\tilde{y})$, defining $M = \rho_w \tilde{v}_w/\rho_e \tilde{u}_e$ and integrating from the edge of the laminar sublayer to any point $\tilde{y}^+ = \tilde{y}u_\tau/\nu_w$, with $\xi = \tilde{u}/\tilde{u}_e$, gives

$$\int_{\xi_s}^{\xi} \frac{d\xi}{[(h/h_w)(C_f + M\xi)]^{1/2}} = \left[(1+m_e)\frac{H_w}{H_e}\right]^{1/2} \frac{1}{K} \ln \frac{\tilde{y}^+}{\tilde{y}_s^+}$$

which can be written, after changing the limits of integration

$$(h_w/h_e)^{-1/2} \int_0^{\xi} \frac{d\xi}{[(h/h_w)(C_f + M\xi)]^{1/2}} = \frac{1}{K} \ln \tilde{y}^+ + \bar{B}$$

where $\bar{B}$ is the empirical "constant"

$$\bar{B} \equiv -\frac{1}{K} \ln \tilde{y}_s^+ + (h_w/h_e)^{-1/2} \int_0^{\xi_s} \frac{d\xi}{[(h/h_w)(C_f + M\xi)]^{1/2}}$$

Whereas in incompressible flow $\bar{B} = 5$, the experiments of Danberg and Squire at supersonic speeds have demonstrated that $\bar{B}$ is a function of M, which can be approximated by the curve fits‡

$$\left.\begin{aligned} &0 \leqq M_e \leqq 3.5: \quad \bar{B} = 5[1 - 0.6 \times 10^3 M(M_e/3.5)]^{3/2} \\ &3.5 \leqq M_e: \quad \bar{B} = 5[1 - 0.6 \times 10^3 M] \end{aligned}\right\} \bar{B} \gtrsim 0$$

Defining§

$$C_1 \equiv [B - (B^2 + 4A^2)^{1/2}]/2A^2, \quad C_2 \equiv [B + (B^2 + 4A^2)^{1/2}]/2A^2$$
$$C_3 \equiv C_f/M, \quad k^2 \equiv (C_2 - C_1)/(C_3 + C_2),$$
$$\sin^2\theta \equiv (C_2 - \xi)/(C_2 - C_1)$$

and since

$$\ln \tilde{y}^+ = \ln y^+ + \ln L/r$$

the compressible law of the wall becomes

$$-2\left[\frac{h_e/h_w}{A^2 M(C_3 + C_2)}\right]^{1/2} [\mathscr{F}(\theta, k) - \mathscr{F}(\theta_{\xi=0}, k)] = (1/K)\ln[(C_f')^{1/2} Re_y] + (1/K)\ln(L/r) + \bar{B} \tag{26}$$

where

$$\mathscr{F}(\theta, k) = \int_0^{\theta} \frac{d\theta}{(1 - k^2 \sin^2\theta)^{1/2}} \tag{27}$$

$$y^+ \equiv y u_\tau/\nu_w = (C_f')^{1/2} Re_y \tag{28}$$

$$Re_y = \frac{\rho_s}{\rho_o}\left(\frac{\rho_o a_o}{\mu_o}\right)\left(\frac{H_e}{H_w}\right)^{(1+\sigma)} (1+m_e)^{-[(3\gamma-1)/2(\gamma-1)]} M_e y \tag{29}$$

For $M = 0$, $k = 0$ the elliptic integrals $\mathscr{F}(\theta, k)$ reduce to arcsin functions, and the law of the wall is given by the Van Driest "generalized" velocity distribution.[10] Evaluating the law of the wall at y_m gives the velocity ratio $(u/u_e)_m = \bar{U}_m$ along the match point. Actually, what we require for matching with the outer layer is the streamwise derivative of $(u/u_e)_m$, which is found by differentiating the law of the wall.[4]

With the velocity profile given by the law of the wall and the enthalpy profile given by the Crocco integral in the inner layer, exact expressions for the stress and heat flux at y_m can be obtained by integrating the momentum and energy equations away from the surface, i.e.,

$$\tau_m - \tau_w = \frac{dp}{dx} y_m + \frac{d}{dx}\int_0^{y_m} \rho u(u - u_m)\, dy + \int_0^{y_m} \rho u\, dy \cdot \frac{du_m}{dx} + \rho_w v_w u_m \tag{30}$$

and

$$(q + u\tau)_m - q_w = \frac{d}{dx}\left[\frac{H_w B}{u_e}\int_0^{y_m} \rho u(u - u_m)\, dy\right] + \int_0^{y_m} \rho u\, dy \cdot \frac{dH_m}{dx} + \left(\frac{H_w B}{u_e}\right)\rho_w v_w u_m \tag{31}$$

‡ Contrary to the data obtained by Danberg,[9] which showed an effect of H_w/H_e on the additive constant $\bar{B}$ in the compressible law of the wall, more recent profile data shows very little, if any, effect of H_w/H_e on $\bar{B}$. The measurements of Laderman and Demetriades[19] at $M_e = 9.4$, $H_w/H_e = 0.38$ and Owen and Horstman[20] at $M_e = 7.2$, $H_w/H_e = 0.47$ show that $\bar{B}$ is virtually unchanged from the incompressible value ($\bar{B} = 5$), while the measurements of Lewis and Gran[21] at $M_e = 4$, $H_w/H_e = 0.35$ show only a slight increase in $\bar{B}$ (to about 5.5). Some of Danberg's data was obtained at values of Re_θ that may not have been sufficient to ensure a fully developed turbulent layer.

§ For large blowing, $\sin^2\theta$ and k^2 are redefined, i.e., $k^2 \equiv (C_3 + C_2)/(C_2 - C_1)$ and $\sin^2\theta \equiv (C_2 - \xi)/(C_2 + C_3)$ so that k^2 is always less than one.

where the integrals in these expressions are evaluated using Eqs. (23) and (26). For example, if

$$J_1 = \int_0^{y_m} \frac{\rho u}{\rho_w u_e} dy \quad \text{and} \quad J_2 = \int_0^{y_m} \frac{\rho u}{\rho_w u_e}\left(\frac{u}{u_e} - \frac{u_m}{u_e}\right) dy$$

then

$$J_i = \frac{K v_w}{u_\tau}\frac{u_e}{u_\tau} e^{-K\bar{B}} \int_0^{\bar{U}_m} \frac{j_i \exp[\alpha f(\xi)]}{(h/h_w)^{3/2}[1+(M/C_f)\xi]^{1/2}} d\xi$$

which can be integrated repeatedly by parts if

$$\alpha = K(u_e/u_\tau), \quad Z = \exp[\alpha f(\xi)]$$

$$f(\xi) = \int_0^{\bar{U}_m} \frac{d\xi}{(h/h_w)^{1/2}[1+(M/C_f)\xi]^{1/2}}, \quad g(\xi) = \frac{j_i}{\alpha(h/h_w)}$$

$$j_i = \xi \text{ for } J_1, \quad j_i = \xi(\xi - \bar{U}_m) \text{ for } J_2$$

to give

$$\int g(\xi)\, dz = \exp[\alpha f(\xi)]\left\{g(\xi) - \frac{g'(\xi)}{\alpha f'(\xi)} + \frac{1}{\alpha^2 f'(\xi)}\frac{d}{d\xi}\left(\frac{g'}{f'}\right) - \cdots\right\} \tag{32}$$

where $(1/\alpha) \sim 0(C_f{}^{1/2}) \ll 1$. By approximating $h/h_w \simeq h_m/h_w$ in $f(\xi)$ and $g(\xi)$ and $1+(M/C_f)\xi \simeq 1+(M/C_f)\bar{U}_m$ in $f(\xi)$, the preceding series truncates with the term $0(\alpha^{-1})$ for J_1, and $0(\alpha^{-2})$ for J_2 so that¶

$$J_1 = \frac{\bar{U}_m y_m}{(h_m/h_w)} - \frac{1}{K}\left(\frac{u_\tau}{u_e}\right)\frac{y_m}{(h_m/h_w)^{1/2}}\left(1+\frac{M}{C_f}\bar{U}_m\right)^{1/2} \tag{33}$$

$$J_2 = -\frac{1}{K}\left(\frac{u_\tau}{u_e}\right)\frac{\bar{U}_m y_m}{(h_m/h_w)^{1/2}}\left(1+\frac{M}{C_f}\bar{U}_m\right)^{1/2} + \frac{2}{K^2}\left(\frac{u_\tau}{u_e}\right)^2 y_m\left(1+\frac{M}{C_f}\bar{U}_m\right) \tag{34}$$

The abovementioned expressions for J_1 and J_2 are the key results for evaluating the stress, heat flux, and mass flux at the outer edge of the inner layer. Inspection of Eqs. (30–34) shows that the stress and heat flux at the match point depend on the streamwise derivatives of mean flow properties at the match point, and the derivative of y_m itself, as well as the derivative of the stress at the surface. The final forms of these differential equations are given in Ref. 4.

Solution of the wall layer for velocity, enthalpy, stress, and heat flux has been obtained analytically in terms of the given wall and edge conditions (M_e, H_w/H_e and M); three "parameters" (y_m, C_f and S_t), and two empirical "constants" (K and $\bar{B}$). By matching this inner solution with an integral moment method for the outer layer, the three "parameters" y_m, C_f and S_t are determined. In addition to u/u_e, H/H_e, τ, and q, $\partial u/\partial y$ and $\partial H/\partial y$ are also matched. These expressions are also given in Ref. 4, along with certain other auxiliary expressions (such as $d\bar{U}_m/dx$, $d\bar{H}_m/dx$, etc.) required for the matching.

IV. Moment Integral Method for Outer Layer

In order to determine the relative scale of the inner and outer layers y_m, and the quantities τ_m and q_m, a moment integral method is used in the outer layer. In this layer independent two-parameter families of profiles are chosen for U and H. The "free" parameters of the profiles are determined implicitly by matching with relations obtained for the inner layer (law of the wall and Crocco integral) for U and H and the lateral and streamwise derivatives of these quantities along the unknown match point y_m. The profiles selected are power laws of the form

$$\bar{U} = U/U_e = 1-(1-\bar{U}_m)(1-\eta)^n, \quad n>0 \tag{35}$$

$$\bar{H} \equiv H/H_e = 1-(1-\bar{H}_m)(1-\eta)^m, \quad m>0 \tag{36}$$

¶ These approximations yield identical results for the leading term of the series as the exact expressions for f and g, and are used here to simplify the task of differentiating J_2.

where $\bar{U}_m$, $\bar{H}_m$, n, and m are free to vary with x. In order for a Crocco integral to exist in the outer layer, m must equal n but, in general, this will not be true. In fact, in terms of the more conventional definitions

$$C_H \equiv -q_w/(H_w-H_e)\rho_e u_e = \frac{2m_e St}{(1+m_e)(1-H_w/H_e)} \tag{37}$$

$$\tilde{C}_f \equiv 2\tau_w/\rho_e u_e{}^2 = 2C_f \tag{38}$$

it is easy to show that a Crocco integral ($m=n$) exists in the outer layer only when the Reynolds analogy holds, i.e., when $C_H = \tilde{C}_f/2$.

In the abovementioned profile families

$$\eta = (Y-Y_m)/\delta \tag{39}$$

where δ is the thickness of the *outer* layer in the transformed coordinate

$$Y - Y_m = \int_{y_m}^{y} \frac{a_e \rho}{a_o \rho_o} dy \tag{40}$$

Because the momentum and energy equations are satisfied exactly in the inner layer using the law of the wall, no new information would be obtained by integrating the conservation equations and velocity moment across the inner layer. The momentum integral, first velocity moment, and energy integral for the outer layer are obtained by integrating the conservation equations from $Y = Y_m$ to $Y = Y_m + \delta$.

Momentum Integral—Outer Layer

$$\left.\begin{aligned} &-\delta A_1 \frac{d\bar{U}_m}{dx} + \delta A_2 \frac{dn}{dx} + I_5 \frac{d\delta}{dx} + (\rho_s/\rho_o)(1+m_e)^{-(\gamma+1)/2(\gamma-1)} \times M(1-\bar{U}_m) \\ &-(1-\bar{U}_m)\left(\frac{1}{\rho_o U_e}\frac{d\dot{m}}{dx}\right) = (E_1 - I_5 - I_2)\frac{\delta}{M_e}\frac{dM_e}{dx} - \left(\frac{a_o}{U_e{}^2 a_e \rho_o}\right)\tau_m \end{aligned}\right\} \tag{41}$$

First Velocity Moment—Outer Layer

$$\left.\begin{aligned} &-\delta A_3 \frac{d\bar{U}_m}{dx} + \delta A_4 \frac{dn}{dx} + I_6 \frac{d\delta}{dx} + (\rho_s/\rho_o)(1+m_e)^{-(\gamma+1)/2(\gamma-1)} \times M(1-\bar{U}_m{}^2) \\ &-(1-\bar{U}_m{}^2)\left(\frac{1}{\rho_o U_e}\frac{d\dot{m}}{dx}\right) = (2E_2 - I_6 - 2I_3)\frac{\delta}{M_e}\frac{dM_e}{dx} - 2\left(\frac{a_o}{U_e{}^2 a_e \rho_o}\right)\tau_m(\bar{U}_m + \alpha_o) \end{aligned}\right\} \tag{42}$$

Energy Integral—Outer Layer

$$\begin{aligned} &-\delta B_3 \frac{d\bar{U}_m}{dx} + \delta B_4 \frac{dn}{dx} + E_4 \frac{d\delta}{dx} + \delta B_1 \frac{d\bar{H}_m}{dx} + \delta B_2 \frac{dm}{dx} \\ &+(\rho_s/\rho_o)(1+m_e)^{-(\gamma+1)/2(\gamma-1)} \times M(1-\bar{H}_m) - (1-\bar{H}_m) \times \left(\frac{1}{\rho_o U_e}\frac{d\dot{m}}{dx}\right) = -E_4 \frac{\delta}{M_e}\frac{dM_e}{dx} - \left(\frac{1}{\rho_o U_e H_e}\right) q_m - \\ &\left(\frac{a_e}{\rho_o a_o H_e}\right)\bar{U}_m \tau_m \end{aligned} \tag{43}$$

where the integral functions A_i, B_i, E_i, and I_i are given in Ref. 4. The equations for $\dot{m}/\rho_o U_e$ and the normalized stress and heat flux at y_m, obtained from the inner layer, are given in Ref. 4. The term involving the integral of the turbulent stress across the outer layer in the velocity moment (the turbulence production) is

$$\alpha_o \equiv \int_0^1 \frac{\tau}{\tau_m}\left(\frac{\partial \bar{U}}{\partial \eta}\right) d\eta \tag{44}$$

On the basis of stability of solutions (Sec. II and VI) we evaluate τ/τ_m in the outer layer as though the density is constant, i.e.,

$$\frac{\tau}{\tau_m} = \left(\frac{\varepsilon}{\varepsilon_m}\right)\frac{(\partial\bar{U}/\partial\eta)}{(\partial\bar{U}/\partial\eta)_m} \tag{45}$$

Since $\varepsilon \to 0$ at the edge of layer, the lateral variation of ε in the outer layer can be approximated by

$$\varepsilon/\varepsilon_m = 1-\eta^\omega \tag{46}$$

where, according to measurements by Bradshaw and the analysis of data for supersonic layers by Maise and McDonald, ω has a value around 2 or 3. On the basis of stability of solutions over a wide range of Mach numbers, we tentatively select the value $\omega = 3$ (see discussion in Sec. II and VI).

Finally, a relation for τ_m is obtained in terms of the eddy viscosity and velocity gradient at the matching point y_m. The length scale for the eddy viscosity is the constant-density displacement thickness

$$\tilde{\delta}_i^* = \int_0^{\tilde{\delta}_e}(1-u/u_e)\,d\tilde{y} \tag{47}$$

and

$$\varepsilon_m = Fu_e\tilde{\delta}_i^*, \qquad F \simeq 0.018 \tag{48}$$

Then, since

$$\tau_m = \rho_m\varepsilon_m(\partial\tilde{u}/\partial\tilde{y})_m$$

and $(\partial\tilde{u}/\partial\tilde{y})_m$ is known from the solution of the inner layer, the normalized stress along y_m is given by

$$\left(\frac{a_o}{U_e^2 a_e\rho_o}\right)\tau_m = (\rho_s/\rho_o)^2(1+m_e)^{-[(\gamma+1)/(\gamma-1)]}\times \frac{F\cdot(\delta_i^*/\delta)a^*n}{[\bar{H}_m+m_e(\bar{H}_m-\bar{U}_m^2)]^2} \tag{49}$$

With the three integral equations for the outer layer, the preceding equation for τ_m, and the matching relations with the inner layer, the system of ordinary differential equations can be integrated downstream. Since the solution of the inner layer involves three "parameters" ($\tilde{C}_f$, S_t, and y_m), and the unknown in the outer layer is δ, these four quantities must be specified at the initial station in order to form all other quantities (n, m, etc.) and all the initial streamwise derivatives. From the equations for J_1 and J_2 in the inner layer and the integral functions in the outer layer one obtains the following:

$$\delta_e = y_m+(\rho_o/\rho_s)(1+m_e)^{(\gamma+1)/2(\gamma-1)}[(1+m_e)E_1-m_eI_2]\delta \tag{50}$$

$$\theta = \frac{\bar{U}_m(1-\bar{U}_m)y_m}{(h_m/h_e)}+\frac{C_f^{1/2}y_m}{K(h_m/h_e)^{1/2}}(2\bar{U}_m-1)\beta_o-(2/K^2)C_f y_m\beta_o^2+(\rho_o/\rho_s)(1+m_e)^{(\gamma+1)/2(\gamma-1)}[I_1-I_2]\delta \tag{51}$$

By specifying $\tilde{C}_f$, C_H, δ_e and θ at the initial station, the above-mentioned expressions and matching conditions are used to calculate the remaining unknowns: y_m, $\bar{U}_m$, δ, m, n, $\bar{H}_m$, and B. These variables are sufficient to determine the initial velocity and enthalpy profiles and all initial streamwise derivatives.

V. Some Computer Results and Experimental Comparisons

By specifying initial values for $\tilde{\delta}_e$, $\tilde{\theta}$, $\tilde{C}_f$, and C_H, and also the unit stagnation Reynolds number, where if $\mu \sim T^\sigma$

$$\rho_o a_o/\mu_o = (u_e/v_e)/(\rho_s/\rho_o)M_e(1+m_e)^{\sigma-[(\gamma+1)/2(\gamma-1)]}$$

Equations (23, 26, 50, and 51) are solved simultaneously to give all the necessary starting conditions. A set of nine nonlinear differential equations is then integrated to give the solution downstream of the initial station. These differential equations are the momentum, first moment, and energy equations for the outer layer, the equation for τ_m from the inner layer, and equations obtained by differentiating the relations for $\bar{U}_m$, $\bar{H}_m$, m, n, and B with respect to x. The method used to solve the system, which is linear when solving for the derivatives, uses gauss elimination with partial pivoting, with an iterative routine to improve the solution. A comparison of this method of solving systems of linear equations with other techniques is given in Ref. 22. For zero pressure gradient, nonadiabatic flows the average computing time on an IBM 360-75 machine is about 15 sec for Re_θ to increase by a factor of 10^2.

Computer results have been obtained and are reported in Ref. 4 for flow over adiabatic and cold walls ($0.05 < H_w/H_e < 1$) up to Mach 10, relaxing flows where $\tilde{C}_f$ and/or C_H are far from their equilibrium values initially (or where M is changed abruptly), boundary layers in strong positive and negative pressure gradients, and flows in which the rate of surface mass injection is determined by a local energy balance at the surface (ablation and transpiration cooling). These have been compared with a number of experiments, including the low-speed results summarized at the AFOSR-Stanford conference.[23] Results are also presented in Ref. 4 for multiple fast expansions and compressions (wavy wall) simulating flow over striation and scallop-type roughness observed on re-entry vehicles. These and more recent calculations have been used to find the phase relations between heating oscillations and surface waves and to find the conditions at which the layer separates along the wavetrain.

An example of the inability of conventional finite-difference methods to account for nonequilibrium effects on turbulence structure is provided by the experiments by Sturek and Danberg[16,17] for flow over a compression ramp at $M_\infty = 3.5$. In these experiments the Mach number decreased from 3.5 to 2.9 over a streamwise distance of 11 boundary-layer thicknesses, which is a fairly moderate pressure gradient. Analysis of the profile data by Sturek[16] showed that in the inner layer values of l/y as large as 0.65 occurred during the compression, compared to the unique value of 0.41 input into finite-difference solutions. Solutions for these experimental conditions using the two-layer model showed that the peak value of l/y in the inner layer, computed from Eq. (19), increased from 0.40 at the start of the compression to 0.59 at the last measuring station on the ramp where $M_e = 2.9$. Moreover, the two-layer model predicted that the peak value of l/δ_e increased from 0.081 to 0.122 (Sturek's data showed an increase from 0.08 to 0.134), whereas this peak value is usually fixed as a unique constant (0.09) in finite-difference methods.

A comparison of the predictions for the skin-friction coefficient with data of Sturek and Danberg is shown in Fig. 1. (Measured velocity profiles for this case are compared with predictions of the two-layer model in Fig. 2.) The finite-difference calculations were performed by Sturek using the computer code of Hixon, Beckwith, and Bushnell.[24] The predicted skin friction falls about

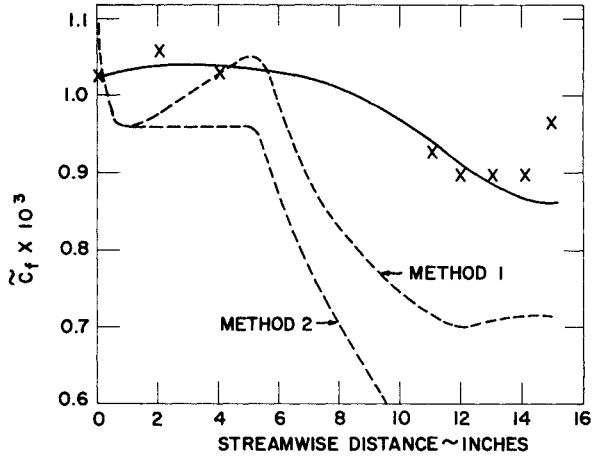

Fig. 1 Distribution of the skin friction in a positive pressure gradient, $M_{e_o} = 3.51$.

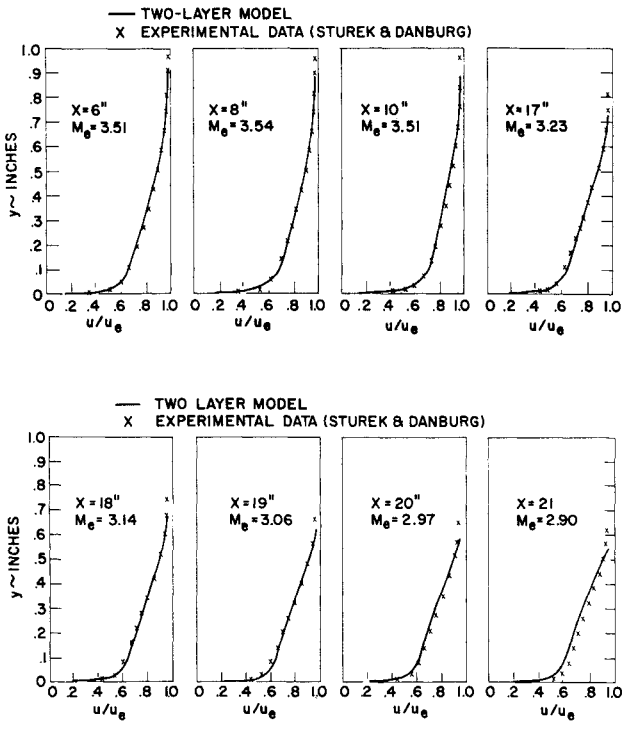

Fig. 2 Velocity profiles in a positive pressure gradient.

23% below the data and below predictions of the two-layer model.** This discrepancy can be shown to become even more significant in more severe pressure gradients, particularly at higher Mach numbers.††

Some results of the two-layer model for highly nonequilibrium flows are shown in Figs. 3 and 4. These calculations were performed in an attempt to simulate (without including inviscid interaction) flow over compression flaps. For these calculations it was assumed that full compression (the downstream pressure corresponding to an isentropic turn to a given flap angle) was complete over streamwise length scales corresponding to various multiples of the approach boundary-layer thickness. Figure 3 shows the effect of flap angle on skin friction at $M_\infty = 8$ for compression lengths of only one and two δ_{e_o}. This is equal to, or

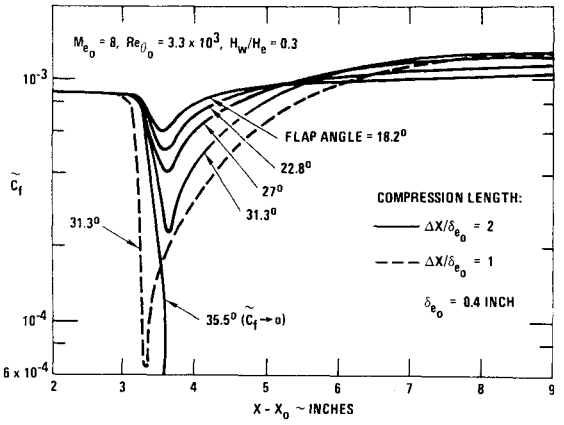

Fig. 3 Distribution of the skin friction for various flap angles.

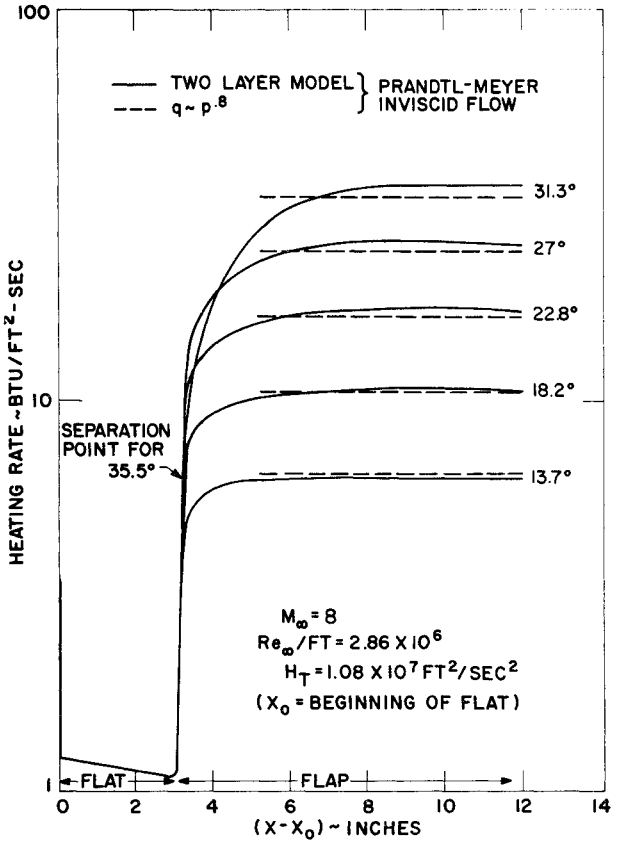

Fig. 4 Distribution of the surface heat flux for various flap angles.

even less than, the interaction length observed experimentally for turbulent boundary layers without separation.[25] The skin friction remains positive for flap angles up to 31.3°, but for an angle of 35.5° $\tilde{C}_f \to 0$ and the layer separates. Thus, the incipient separation angle is predicted to occur between these two angles, which is in agreement with the data of Elfstrom[25] and Holden[26] obtained at about Mach 9. The effect of the length of compression on $\tilde{C}_f$ can be seen by comparing the solutions for a flap angle of 31.3°.

The predicted heating distributions show several interesting features. First, as expected, there is a catastrophic failure of the Reynolds analogy (the heating increases rapidly despite the drop in $\tilde{C}_f$). (The Crocco integral for the enthalpy profiles also breaks down in this region.) Second, the heating continues to rise after the end of the compression at $(x - x_o) = 3.4$, revealing strong nonequilibrium relaxation effects downstream of rapid compressions. Third, in the equilibrium flow far downstream of the compression the theory predicts that $q \sim p^{0.8}$ scaling is remarkably good for all flap angles. (Of course, these results do not include entropy layer swallowing effects produced by the curved compression shock, which, in some cases, can give rise to sharp heating peaks on the flap.) Results for fast expansions (biconic shapes) at hypersonic speeds are given in Ref. 4.

VI. Conclusions

All results reported here have been obtained by evaluating the turbulent production integral over the outer layer using a cubic variation of ε between y_m and δ_e [$\omega = 3$ in Eq. (46)]. Stable solutions, in the sense that the power-law exponent n in the outer layer velocity profile remains bounded, have been obtained for negative and positive pressure gradients, with cold and adiabatic walls, up to Mach 10. It is really quite remarkable that the evaluation of the production integral with a simple cubic variation of ε produces stable solutions for such a wide range of flow conditions. For incompressible flow in zero pressure gradient, for example, a constant value of the production integral

** An altered mixing length distribution tried by Sturek gave even worse results for $\tilde{C}_f$.

†† On the other hand, these strong pressure induced nonequilibrium effects are less important in incompressible flows. Global interaction with the inviscid flow limits the severity of a positive pressure gradient that can be impressed on the layer.

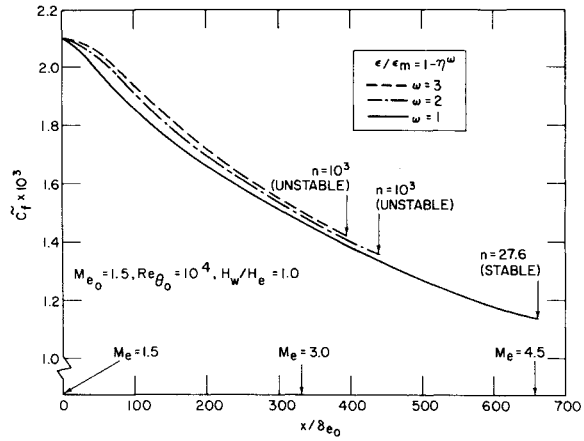

Fig. 5 Skin-friction distributions in a negative pressure gradient with various values of ω in turbulent production integral.

$\alpha_o = 0.18$ gives a downstream solution of the type $n \to \infty$, while a value $\alpha_o = 0.09$ gives a solution in which $n \to 0$. Moreover, these instabilities occur after a streamwise distance of only about ten boundary-layer thicknesses. Despite this rather sensitive dependence of the streamwise variation of n on the magnitude of α_o, the values of $\tilde{C}_f$ along the integral curves differ by less than 1% for $\alpha_o = 0.18$ and $\alpha_o = 0.09$. Clearly then, the stability of the interaction between the inner and outer layers is much more sensitive to the level of turbulence production in the outer layer than is the streamwise development of the layer as a whole. In other words, as long as a way of calculating α_o can be found which keeps the inner-outer layer interaction stable (n finite), the results for $\tilde{C}_f(\tilde{x})$, $\theta(\tilde{x})$, etc., should be within a few percent of the results of all other stable solutions obtained with slightly different methods of calculating α_o. This is true whether α_o is computed using eddy viscosity or other, more sophisticated, stress models.

Solutions for boundary layers in sustained expansions have exhibited instabilities of the type $n \to \infty$ for $\omega = 3$ so that the cubic variation of $\varepsilon/\varepsilon_m$ obviously cannot be considered "universal." Because for this type of instability ($n \to \infty$) α_o, and hence ω, must be decreased to produce stable solutions, a quadratic or even linear variation of $\varepsilon/\varepsilon_m$ across the outer layer may be required. An example of the unstable behavior in a sustained expansion is shown in Fig. 5. The calculations were performed for a flow in which the inviscid Mach number increases linearly from 1.5 to 4.5 over a streamwise distance equal to 660 times the initial boundary-layer thickness. Solutions were performed for $\omega = 1$, 2 and 3, starting with an initial boundary layer in equilibrium for zero pressure gradient at $Re_\theta = 10^4$. As indicated in the figure, n grows to 10^3 for $\omega = 3$ and 2 at $x/\delta_{e_o} = 390$ and 430, respectively. Both solutions are unstable with n increasing exponentially at these values of x. The solution for $n = 1$ is stable throughout the expansion, with $n = 27.6$ at the end of the run. Despite the wide difference in the stability characteristics of the solutions, Fig. 5 shows that the maximum difference in $\tilde{C}_f$ along the integral curves for the three values of ω is only about 4%. A stable solution is found by lowering the value of ω (decreasing α_o) from 3 to 1 but the effect of this operation on the boundary-layer solution is practically negligible. Consequently, it appears that the two-layer model can provide quantitative results for the streamwise variation of the turbulence production in the outer layer simply on the basis of the stability of the inner-outer layer interaction.

References

[1] Lewis, J., Gran, R., and Kubota, T., "An Experiment on the Adiabatic Compressible Turbulent Boundary Layer in Adverse and Favorable Pressure Gradients," *Journal of Fluid Mechanics*, Vol. 51, 1972, pp. 657–672.

[2] Coles, D., "The Law of the Wake in the Turbulent Boundary Layer," *Journal of Fluid Mechanics*, Vol. 1, 1956, pp. 191–226.

[3] Maise, G. and McDonald, H., "Mixing Length and Kinematic Eddy Viscosity in a Compressible Boundary Layer," *AIAA Journal*, Vol. 6, No. 1, Jan. 1968, pp. 73–80.

[4] Reeves, B., "A Two-Layer Model of High-Speed, Two- and Three-Dimensional Turbulent Boundary Layers with Pressure Gradient, Surface Mass Injection and Entropy Layer Swallowing," Pt. 1, Vol. 1, AVSD-0474-71, 1973, Avco Systems Div., Wilmington, Mass.; also "Turbulent Flow about Conical Bodies at Large Angle of Attack," Vol. 1, AVSD-0200-73, 1973, Avco Systems Div., Wilmington, Mass.

[5] Lewis, J. E., Kubota, T., and Webb, W., "Transformation Theory for the Compressible Turbulent Boundary Layer with Arbitrary Pressure Gradient," SAMSO-TR-68-439, Sept. 1968, Space and Missiles System Organization, U.S. Air Force.

[6] Nee, V. and Kovasznay, L., "Single Phenomenological Theory of Turbulent Shear Flows," *Physics of Fluids*, Vol. 12, 1969, pp. 473–484.

[7] Bradshaw, P. and Ferriss, D., "Calculation of Boundary Layer Development Using the Turbulent Energy Equation," *Journal of Fluid Mechanics*, Vol. 46, 1971, pp. 83–110.

[8] Squire, L. C., "A Law of the Wall for Compressible Turbulent Boundary Layers with Air Injection," *Journal of Fluid Mechanics*, Vol. 37, 1969, pp. 449–456.

[9] Danberg, J. E., "Characteristics of the Turbulent Boundary Layer with Heat and Mass Transfer at M = 6.7," NOLTR Rept. 64-99, Oct. 1964, Naval Ordnance Lab., White Oak, Silver Spring, Md.

[10] Van Driest, E. R., "On Turbulent Flow Near a Wall," *Journal of the Aeronautical Sciences*, Vol. 23, 1956, pp. 1007–1011.

[11] Smith, A. M. O. and Cebeci, T., "Numerical Solution of the Turbulent Boundary Layer Equations," Rept. DAC 33735, May 1967, McDonnell Douglas Corp., St. Louis, Mo.

[12] Herring, H. J. and Mellor, G. L., "A Method of Calculating Compressible Turbulent Boundary Layers," CR-1144, Sept. 1968, NASA.

[13] Clauser, F., "The Turbulent Boundary Layer," *Advances in Applied Mechanics*, Vol. 4, Academic Press, New York, 1956, pp. 1–51.

[14] Bradshaw, P. and Ferriss, D., "The Response of a Retarded Equilibrium Turbulent Boundary Layer to the Sudden Removal of Pressure Gradient," Rept. 1145, 1965, National Physics Lab., London, England.

[15] Glowacki, W. and Chi, S., "Effect of Pressure Gradient on Mixing Length for Equilibrium Turbulent Boundary Layers," AIAA Paper 72-213, Washington, D.C., 1972.

[16] Sturek, W., "Turbulent Boundary-Layer Shear Stress Distributions for Compressible Adverse Pressure Gradient Flow," *AIAA Journal*, Vol. 12, No. 3, March 1974, pp. 375–376.

[17] Sturek, W. and Danberg, J., "Supersonic Turbulent Boundary Layer in Adverse Pressure Gradient, Pt. I: The Experiment," *AIAA Journal*, Vol. 10, No. 4, April 1972, pp. 475–480; "Pt. II: Data Analysis," *AIAA Journal*, Vol. 10, No. 5, May 1972, pp. 630–635.

[18] Antonia, R. and Luxton, R., "The Response of a Turbulent Boundary Layer to a Step Change in Surface Roughness," Pt. 1: "Smooth to Rough," *Journal of Fluid Mechanics*, Vol. 48, 1971, pp. 721–761; Pt. 2: "Rough to Smooth," *Journal of Fluid Mechanics*, Vol. 53, 1972, pp. 737–757.

[19] Laderman, A. and Demetriades, A., "Mean Flow Measurements in a Hypersonic Turbulent Boundary Layer," Rept. U-4950, 1971, Philco-Ford Corp., Newport Beach, Calif.

[20] Owen, F. and Horstman, C., "On the Structure of Hypersonic Turbulent Boundary Layers," *Journal of Fluid Mechanics*, Vol. 53, 1972, pp. 611–638.

[21] Lewis, J., private communication, 1971, TRW Systems Division, Redondo Beach, Calif.

[22] Fitzgerald, K. E., "Error Estimates for the Solution of Linear Algebraic Systems," *Journal of Research of the National Bureau of Standards, B. Mathematics and Mathematical Physics*, Vol. 74B, 1970, pp. 251–310.

[23] Kline, S., Morkovin, M., Sovran, G., and Cockrell, D., *AFOSR-IFP, Stanford Conference on Turbulent Boundary Layers*, Stanford Univ. Press, Stanford, Calif., 1968.

[24] Hixon, B., Beckwith, I., and Bushnell, D., "Computer Program for Compressible Laminar or Turbulent Nonsimilar Boundary Layers," TM X-2140, 1971, NASA.

[25] Elfstrom, G., "Turbulent Separation in Hypersonic Flow," Aero Rept. 71-16, Sept. 1971, Imperial College, London, England.

[26] Holden, M., "Shock Wave-Turbulent Boundary-Layer Interaction in Hypersonic Flow," AIAA Paper 72-74 San Diego, Calif., 1972.